JOURNAL OF THERMOPHYSICS AND HEAT TRANSFER
Vol. 22, No. 3, July–September 2008

Experimental Study of Graphite Ablation in Nitrogen Flow

Toshiyuki Suzuki* and Kazuhisa Fujita†
Japan Aerospace Exploration Agency, Tokyo 182-0012, Japan
and
Keisuke Ando‡ and Takeharu Sakai§
Nagoya University, Aichi 464-8603, Japan

DOI: 10.2514/1.35082

The speed of nitridation reaction at a graphite surface is evaluated in an inductively coupled plasma heated wind tunnel. A high-temperature nitrogen plasma flow is generated and a graphite rod is heated by the high-temperature nitrogen flows in the test section of the wind tunnel. The amount of mass loss and the surface temperature of the graphite rod are measured during the experiments. The value of the atomic nitrogen number density striking onto the graphite rod is estimated by calculating the flowfield around the graphite rod without accounting for the nitridation at the graphite surface. The speed of nitridation is deduced from the amount of mass loss rate, the surface temperature, and the atomic nitrogen number density. The results show that the speed of nitridation reaction is about 0.003 for the surface temperature of about 1900 K. The uncertainties in the results are discussed and improvements are proposed.

Nomenclature

A = surface area of graphite test piece, 2.43×10^{-4} m^2
k = surface reaction velocity, m/s
M_s = molecular weight of species s, kg/mol
R = universal gas constant, 8.314 J/(mol · K)
r = mass loss rate, kg/s
T = temperature, K
α = speed of reaction or reaction probability
ρ_s = density of species s, kg/m^3

I. Introduction

WHEN an entry capsule enters into the Earth's atmosphere with a very high speed, such as the atmospheric reentry along a hyperbolic trajectory returning from an outer planet, a strong detached shock wave is formed around the entry capsule. As a result, the flow temperature in the shock layer becomes so high that air molecules can be nearly totally dissociated. Because the entry capsule is exposed to significant aerodynamic heating during such atmospheric entry, a carbon fiber reinforced plastic (CFRP) ablator has frequently been used as a thermal protection system (TPS) of the entry capsule. Based on recent theoretical studies, in which the heating environments over the Stardust entry capsule and the HAYABUSA entry vehicle are analyzed [1,2], the recombination processes of the atomic species behind a shock wave are so slow that a lot of atomic species in the boundary layer can reach the ablating surface. Because the surface of the ablative material could be nearly pure carbon due to a pyrolysis process [3] in such an environment, it is necessary to know how fast the solid carbon on the surface is recessed by the surface reactions, such as oxidation by atomic oxygen or nitridation by atomic nitrogen. Especially, it is important to evaluate the speed of the nitridation reaction that occurs at the ablating surface, because a large amount of atomic nitrogen could reach the ablator surface as compared with that of atomic oxygen in the hyperbolic entry case.

The rate of the nitridation reaction that occurred at the solid carbon in a high-temperature gas flow has been unknown, though the rate of the oxidation reaction associated with ablation is relatively well known [4–7]. Recently, Park and Bogdanoff experimentally determined the speed of the nitridation reaction [8]:

$$\mathrm{N} + \mathrm{C(s)} \rightarrow \mathrm{CN} + 0.35\ \mathrm{eV} \tag{1}$$

The speed of the nitridation is expressed by a reaction probability, which is defined as the ratio of the mass flux of nitrogen contained in the reaction product to the mass flux of nitrogen onto the carbon surface. In the experiment, a highly dissociated nitrogen flow was produced in a shock tube. A grid of metal wire coated with carbon was exposed to the dissociated nitrogen flow, and the CN radiation in the wake of the grid of the metal wire was measured. The radiation emission spectrum of CN was calculated by using a radiation code named NEQAIR [9]. The CN number density was deduced by comparing the emission spectrum between measurement and calculation, through an existing formula obtained by the kinetic theory. The obtained reaction probability was about 0.3.

The accuracy of the reaction probability obtained by Park and Bogdanoff [8] is not examined in the high-enthalpy aerothermal environment produced in a so-called high-enthalpy wind tunnel, such as an arcjet wind tunnel or an inductively coupled plasma (ICP) wind tunnel, which is used for the testing of heat shield materials. Besides, the reaction probability so obtained depends strongly on the accuracy of the radiation modeling. Even though the radiation model has been widely accepted and has been validated against existing experimental data, a further experimental study associated with the nitridation reaction on a carbon surface would be warranted to check the validity of their value.

The present study aims to evaluate the speed of nitridation by using an ICP wind tunnel at the Institute of Aerospace Technology (IAT) of the Japan Aerospace Exploration Agency (JAXA). The high-temperature nitrogen stream is produced by the wind tunnel, and a graphite test piece is heated in the high-temperature nitrogen

Presented as Paper 4402 at the 39th AIAA Thermophysics Conference, Miami, FL, 25–28 June 2007; received 11 October 2007; revision received 24 February 2008; accepted for publication 25 February 2008.

*Researcher, Institute of Aerospace Technology, 7-44-1 Jindaiji Higashi-machi, Chofu-shi, Tokyo 182-8522; suzuki.toshiyuki@jaxa.jp. Member AIAA.

†Senior Researcher, Institute of Aerospace Technology, 7-44-1 Jindaiji Higashi-machi, Chofu-shi, Tokyo 182-8522. Member AIAA.

‡Graduate Student, Department of Aerospace Engineering, Furo-cho, Chikusa-ku, Nagoya.

§Assistant Professor, Department of Aerospace Engineering, Furo-cho, Chikusa-ku, Nagoya. Member AIAA.

flow. The speed of nitridation is estimated from the amount of mass loss of the graphite test piece during the heating test, the surface temperature, and the density of atomic nitrogen reaching the graphite surface. The mass loss is given by

$$r = \frac{M_C}{M_N} A \rho_N k \tag{2}$$

where A denotes the surface area of test piece. The symbol k denotes surface reaction velocity and is given by

$$k = \frac{\alpha}{4} \sqrt{\frac{8RT}{\pi M_N}} \tag{3}$$

where α and T denote speed of reaction and surface temperature, respectively. Note that the speed of reaction is identical to the reaction probability in the kinetic theory. A set of experimental data associated with the preceding formulation is presented in the present study.

It is very likely that the level of the impurities, especially for molecular oxygen concentration, is set to be extremely low before testing. Thus, the mass loss data presented in this study will be free from the mass loss by oxidation. This point will be explained later.

A graphite test piece must be exposed to a higher heat flux to generate the nitridation process with the available power of the ICP wind tunnel (110 kW). Hence, a graphite rod with a small nose radius is chosen in the present study for the test pieces. When the speed of nitridation at the graphite rod is evaluated through Eqs. (2) and (3) from the experimental data, the surface temperature and the area of the surface need to be nearly constant during testing. Main efforts will be elaborated in this study to check whether this requirement is satisfied by operating the wind tunnel for a broader range of operating conditions.

It is difficult to measure the amount of atomic nitrogen striking on the graphite surface. Therefore, the mass fraction of atomic nitrogen striking on the surface will be determined by a numerical simulation. In the numerical simulation, the flowfield over the graphite rod is calculated by accounting for the nitridation process on the test piece. Such a calculation will be possible by modifying an existing computational method, which was originally developed to analyze the thermal response of a charring ablator in an arcjet wind tunnel [3]. In this method, the thermal response of the ablator is calculated in a fully coupled manner with an arcjet freestream, which is predicted by using a computational method [3]. A nitridation process was included in the past calculation, and the mass fraction of the atomic nitrogen was different between, with and without accounting for the nitridation process. Although the numerical procedure in the past work is believed to be more reliable in this regard, the mass fraction of atomic nitrogen is calculated in this study without accounting for the thermal response of the graphite rod. The speed of nitridation is preliminarily estimated based on the mass fraction so calculated for reference. For such a detailed calculation, a thorough diagnosis of the high-temperature nitrogen flow generated by the ICP wind tunnel will be needed. Such an experimental effort is being carried out [10,11], including the operating conditions considered in the present study. The obtained speed of nitridation by using a more detailed numerical approach will be reported in a future paper.

II. Experimental Configurations

The schematic diagram of the 110 kW ICP heated wind-tunnel facility in IAT of JAXA is given in Fig. 1. The facility consists mainly of a plasma torch and a test chamber. The plasma torch is made of a quartz cylindrical tube with an induction coil of three turns. The quartz tube has a diameter of 75 mm and a length of 250 mm. The wind tunnel is usually operated at a frequency of 1.78 MHz by water cooling the quartz tube.

A pure nitrogen gas is used to observe the nitridation reaction that occurs at the graphite surface. Because impurities such as oxygen and hydrogen could moderately affect the mass loss of the graphite

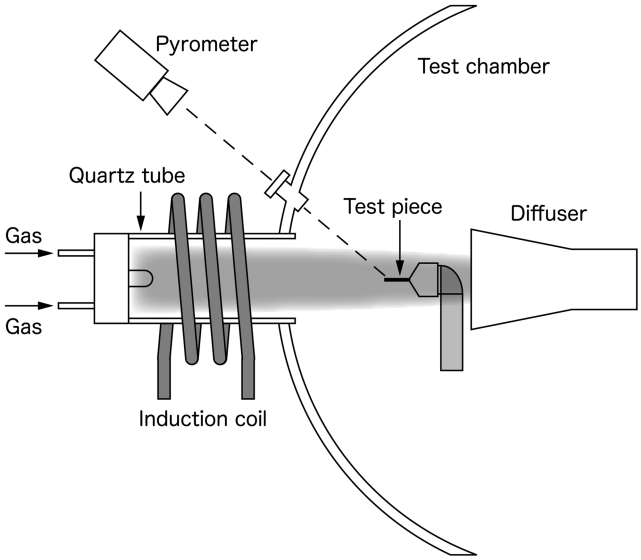

Fig. 1 Schematic of 110 kW ICP heated wind-tunnel facility installed in IAT of JAXA.

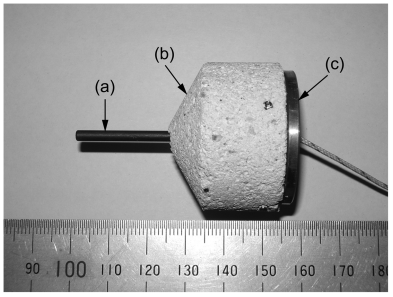

Fig. 2 Photograph of test piece used in the heating test: a) graphite test piece, b) firebrick attachment, and c) interface plate made of copper.

material, the test chamber needs to be evacuated until the level of the impurities is as low as possible. As pointed out by Fujita et al. [10], however, the evacuating system was not able to remove such impurities to a satisfactory level for the purpose of the present study. Therefore, before each of the wind-tunnel operations, the test chamber is filled with nitrogen gas at once, and the chamber is evacuated after that. This "replacement" is repeated three times (pressure ratio = 30). By conducting this replacement, the amount of impurities in the test chamber could become lower by about $(1/30)^3 = 1/27000$ than those without conducting the replacement. A radiation spectroscopic study is being carried out to quantify the amount of the impurities after the replacement [11]. Although the result will not be given in the present paper, the effect of the oxidation reaction to the mass loss data presented in this study is believed to be small based on the spectroscopic data.

A photograph of the test piece used in the heating tests is shown in Fig. 2. A flat-faced graphite rod is mounted on a firebrick attachment. To observe the nitridation phenomenon clearly, it would be better to raise the ratio of the surface area to the volume of the graphite. In addition, the diameter of the graphite rod needs to be as small as possible because the core diameter of the freestream produced by the ICP wind tunnel is believed to be small. For these reasons, the diameter and the length of the graphite rod is chosen to be 3 and 50 mm, respectively. The length of the graphite rod that is exposed to hot nitrogen gas is 25 mm, leading to a surface area of 2.43×10^{-4} m^2. In advance of the heating tests, the moisture content of the graphite test pieces is removed by heating the pieces in an inert gas environment at a constant temperature of 300°C for 3 h. Test conditions and the wind-tunnel operational parameters are summarized in Table 1. The working power used in this study ranges from 70 to 110 kW, and the mass flow rate of working gas is

Table 1 ICP wind-tunnel test conditions

Test piece no.	1	2	3	4	5	6	7	8	9	10
Working gas	N_2	N_2	N_2	N_2	N_2	N_2	N_2	N_2	N_2	N_2
Working power, kW	70	70	70	70	90	90	90	110	110	110
Mass flow rate, g/s	2	2	2	2	2	2	2	2	2	2
Ambient pressure, kPa	10	10	10	10	10	10	10	10	10	10
Heat flux, MW/m^2	0.7	0.7	0.7	0.7	1.1	1.1	1.1	1.4	1.4	1.4
Mass-averaged enthalpy, MJ/kg	15	15	15	15	18	18	18	20	20	20
Exposure time, s	600	900	900	1200	300	600	900	175	300	600

2 g/s, realizing a mass-averaged enthalpy ranging from 15 to 20 MJ/kg. The mass-averaged enthalpy values are determined by using an energy balance method. The heat flux is measured using a Gardon gauge. The forefront of the test piece is placed at 566 mm from the quartz tube exit.

During the heating test, the surface temperature at the nose tip of the graphite is measured by using a one-color optical pyrometer (MIKRON®M90V, Mikron Instrument Co., Inc.). The pyrometer is placed at 750 mm from the graphite test piece. Because the field of view of this pyrometer is 1/5 deg (ϕ 3 mm at a distance of 900 mm), the spatial accuracy is believed to be high enough for the purpose of the present study. A spectral response of the pyrometer is 650 nm. Because CN emits radiation near this wavelength, the emission may introduce some error in the measured temperature. The effect of the CN radiation in the red and near-infrared region was examined by calculating the radiative transport along the path from the graphite surface to the pyrometer. The flow properties along the path were taken from the flowfield solutions obtained by accounting for the CN production due to nitridation. The result shows that there is only small difference of the radiative heat flux between the two cases with and without CN. Thus, the effect of the CN radiation is believed to be small in our temperature measurements.

III. Numerical Methods

Two computational blocks are built to calculate the flowfield in the ICP heated wind tunnel: 1) simulation of the entire flowfield in the plasma torch, and 2) simulation of the flowfield over a graphite test piece in the test chamber. The methodologies are briefly explained next.

A. Flowfield in Plasma Torch

The ICP wind-tunnel flowfield is calculated using a computational fluid dynamics (CFD) technique. An axisymmetric viscous flow is assumed to be in thermochemical equilibrium. A five chemical species model (N, N^+, N_2, N_2^+, and e−) is employed to account for high-temperature phenomena. Mass, momentum, and total energy conservation equations are solved using a finite volume method. Solutions are obtained by numerically integrating the equations in time to steady state. Mass flow rate, working power, and operating frequency are specified as the input for a computation. On the right-hand side of the momentum and energy equations, the Lorentz force and Joule heating terms are included. The axisymmetric electromagnetic field is assumed in the present calculation. Time-averaged values of Lorentz force and Joule heating are calculated by solving Maxwell equations. The Lorentz force and Joule heating terms are updated every 1000 times in the CFD calculation. The details of the numerical method are given in [12].

Figure 3 shows the computational grids used in the present study. Two different computational meshes are used to calculate the ICP flowfield: one for the flowfield calculation denoted by zone 1, and the other for the electromagnetic field given in zone 2, respectively. Each of the number of grid points for zone 1 and zone 2 is 90×44 and 128×63, respectively. The far-field boundary for the computational mesh of the electromagnetic field is extended appropriately to impose the boundary condition: the electrical and magnetic field is taken to be zero at the far-field boundary. The grid system denoted by zone 3 is used for the flowfield computation around the graphite material.

B. Flowfield in Test Chamber

The thermochemical nonequilibrium CFD code developed earlier [2] for air is modified to compute the dissociating and partially ionizing nitrogen flowfield over the graphite test piece. The governing equations are the Navier–Stokes equations for axisymmetric flowfield, consisting of species mass, momentum, total energy, and vibronic energy conservation equations. The equations are discretized by the cell-centered finite volume scheme using AUSM-DV numerical flux [13] and the MUSCL approach for attaining higher-order spatial accuracy. Solutions are obtained by integrating the equations in time to steady state using the LU-SGS algorithm. We employ the five chemical species (N, N^+, N_2, N_2^+, and e−) to be consistent with the plasma torch calculation. A Park's two-

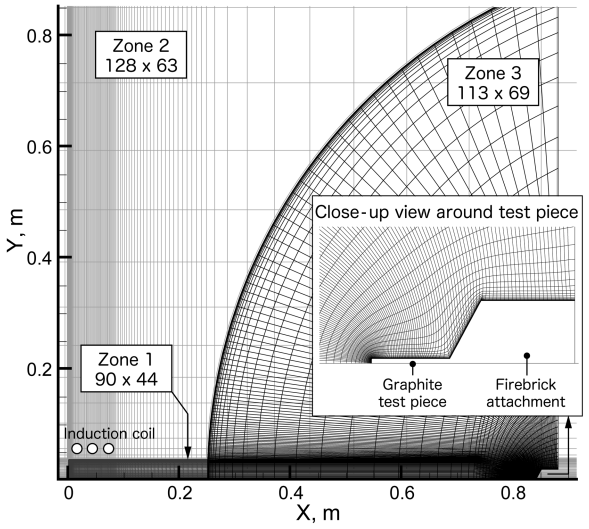

Fig. 3 Computational meshes for ICP wind tunnel: zone 1 for plasma torch flowfield, zone 2 for electromagnetic field, zone 3 for flowfield in the test chamber.

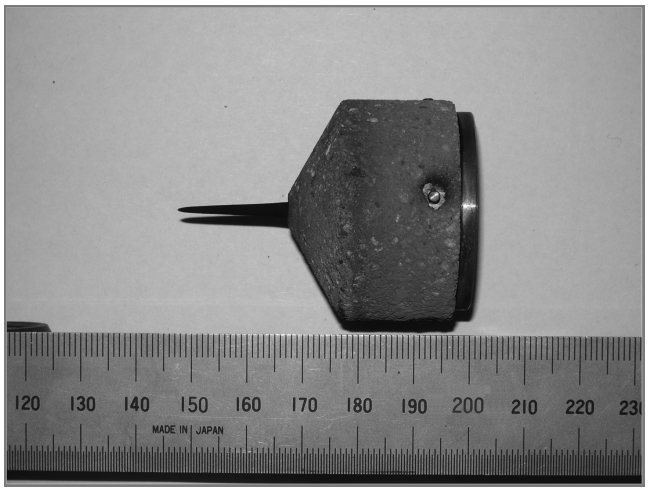

Fig. 4 Photograph of test piece no. 1 after the heating test; working power of 70 kW and exposure time of 900 s.

temperature model is employed to determine the thermochemical nonequilibrium state in the flowfield. Other numerical details are given in our previous papers [2,3] and are omitted here.

A typical example of computational mesh for the flowfield over the test piece is given as zone 3 in Fig. 3. The number of grid points used is 113×69. The inlet boundary condition at the entrance of test chamber is given by the solution obtained by the plasma torch flowfield analysis. As to the wall boundary condition at the wall surface of test piece, the constant wall temperature is arbitrarily chosen as 500 K. The effect of the wall temperature on the number density of the nitrogen species on the surface is small in the present study, as will be shown later. Because the surface catalytic recombination of atomic nitrogen has never been seen experimentally, as mentioned in [14], the wall surface of graphite is assumed to be noncatalytic.

In the present study, the thermochemical nonequilibrium CFD code is parallelized with OpenMP directives. All the flowfield calculations are performed using the CFD code on four processors of Dell Precision 690. Approximately 100,000 iteration steps are needed to drop the L2-norm of the residual three orders of magnitude, requiring about 8 h of CPU time.

IV. Results

A. Experimental Results

1. Shape Change

The heating tests using the graphite rod are conducted in the 110 kW ICP wind tunnel for the wind-tunnel test conditions shown in Table 1. Figure 4 shows a photograph of the test piece after the heating test for case no. 7. By comparing this with the photograph given in Fig. 2, one can see that the graphite rod after the heating test tapers to sharp point, and becomes shorter than the one before heating. This shape change is because the graphite rod receded due to the nitridation reaction that occurred at the surface. After the heating tests, we observed the surface of the graphite test piece using a scanning electron microscope. We did not find any evidence of mechanical erosion at the graphite surface. In addition, the surface on the graphite rod receded by keeping the axisymmetric shape of the rod. The trend is similar for other tested specimens. From these results, we believe that the mass loss of the graphite test piece observed in this study is mainly attributed to the nitridation reaction.

Because of this shape change, the surface area of the graphite rod is varied moderately. A minimum surface area of the graphite rod is obtained for case no. 7 and is found to be about one-half smaller than the initial value of the surface area. For each of the graphite rods tested in the present study, the surface area varied from 95/100 to one-half compared with the initial shape.

2. Surface Temperature

Figure 5 shows the time histories of the measured surface temperature for case nos. 1–4. In these cases, the wind tunnel is operated for the nominal electrical power input of 70 kW. Because a similar trend is seen for the cases of 90 and 110 kW, the results are omitted here. As shown in this figure, the surface temperatures are within a range of 1700–2000 K. A regression analysis is made based on the measured data, and the results are presented in the same figure. From the regression lines, average temperatures are estimated to be 1953, 1930, 1853, and 1822 K, respectively. The temperature rise rate is approximately 4.8 K/ min. A maximum error in the average temperature is estimated to be less than $\pm 3\%$. Therefore, the temperature of graphite test piece is assumed to be constant during the heating test. In the present study, the average temperature values are used to estimate the speed of nitridation of the graphite test piece.

The surface temperature is believed to be unchanged over the surface exposed to the freestream, although the measurement of the surface temperature is made at the tip of the graphite rod. Though the result is not shown here, a heat conduction analysis was made to examine the temperature distribution in the spanwise direction within the material by solving the heat conduction equation. The result shows that the temperature distribution is nearly constant. This trend is due to the fact that the thermal conductivity of the graphite used in the present study is relatively high and the thermal conduction is sufficiently fast for the scale of the material used. It should be noted that the thermomechanical properties of the graphite used in the present study are isotropic.

3. Mass Loss

After the heating tests, graphite test pieces were removed from the firebrick attachments and were weighed to obtain the amount of mass loss of the graphite test piece. Because the surface temperatures are nearly constant in time during testing, the rate of mass loss of a graphite test piece is believed to be a linear function of time except for the beginning of exposure. Thus, mass loss rates are calculated by dividing the measured mass losses by the exposure time. Obtained results are summarized in Table 2.

Figure 6 shows the amount of mass loss of a graphite rod as a function of exposure time. As shown in Fig. 6, the amount of mass loss of a graphite test piece increases with time, as expected. Note that the amount of mass loss for case no. 2 is larger than that for case no. 3, though both test pieces are heated for 900 s with a power input of 70 kW. This difference of the mass loss is due to the fact that the surface temperature for case no. 2 is higher than that for case no. 3, as was shown in Fig. 5. As a result, the mass loss rate for case no. 2 becomes larger than that for case no. 3.

The mass loss rates are plotted against square root of average surface temperature in Fig. 7. From the figure, one can see that the mass loss rate of graphite increases almost linearly with the square root of temperature. This trend is because the mass loss rate is dictated by the square root value of surface temperature, as was shown in Eq. (3). This result also indicates that the present measurements for all wind-tunnel conditions were made in a reaction-rate-controlled regime, because the mass loss rate increases with surface temperature. In this regime, the speed of nitridation is dominated by the surface reaction velocity given by Eq. (3). If the measurements were made at higher surface temperatures, the mass loss rate might become constant, because the speed of nitridation could be controlled by the diffusion velocity of atomic nitrogen.

B. Numerical Results

Calculations are made for three different operating conditions of working power of 70, 90, and 110 kW. A mass flow rate is fixed to be 2 g/s in the calculations. Because a similar trend is seen for the three cases, the calculated result for the case of 90 kW is presented here.

Figure 8 shows a typical example of the converged solution. In the figure, the temperature contours inside the plasma torch and the test chamber (zones 1 and 3) are shown. Because of the significant heating in the plasma torch, the temperature becomes larger than

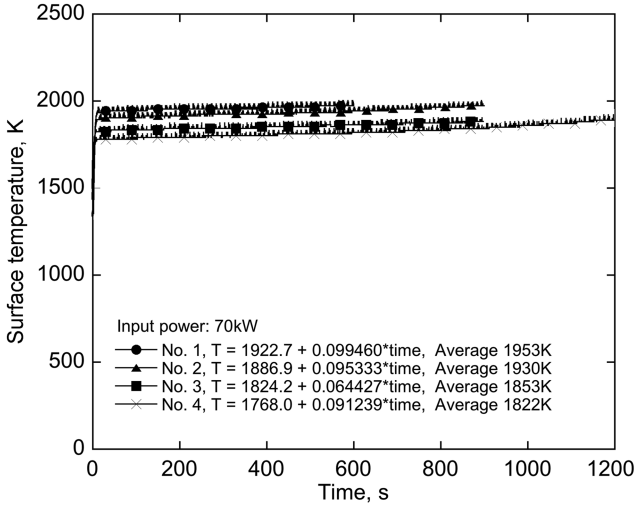

Fig. 5 Time history of surface temperature at the stagnation point for the case of working power of 70 kW.

Table 2 Mass loss of graphite test pieces

Test piece no.	1	2	3	4	5	6	7	8	9	10
Working power, kW	70	70	70	70	90	90	90	110	110	110
Exposure time, s	600	900	900	1200	300	600	900	175	300	600
Average temperature, K	1953, ±3%	1930, ±3%	1853, ±3%	1822, ±3%	2184, ±3%	2075, ±3%	2160, ±3%	2160, ±3%	2139, ±3%	2080, ±3%
Mass before heating, $\times 10^{-1}$ g	6.475	6.478	6.419	6.459	6.418	6.407	6.352	6.422	6.405	6.442
Mass after heating, $\times 10^{-1}$ g	5.058	4.447	4.609	4.240	5.453	4.547	3.917	5.848	5.358	4.421
Mass loss, $\times 10^{-4}$ kg	1.417	2.031	1.810	2.219	0.965	1.860	2.435	0.574	1.047	2.021
Mass loss, %	21.88	31.35	28.20	34.36	15.04	29.03	38.33	8.94	16.35	31.27
Mass loss rare, $\times 10^{-7}$ kg/s	2.362	2.257	2.011	1.849	3.217	3.100	2.706	3.280	3.490	3.368
Speed of nitridation, $\alpha \times 10^{-3}$	3.21, −2% ~ 103%	3.05, −2% ~ 103%	2.80, −2% ~ 103%	2.56, −2% ~ 103%	3.03, −2% ~ 103%	3.00, −2% ~ 103%	2.55, −2% ~ 103%	2.59, −2% ~ 103%	2.78, −2% ~ 103%	2.71, −2% ~ 103%

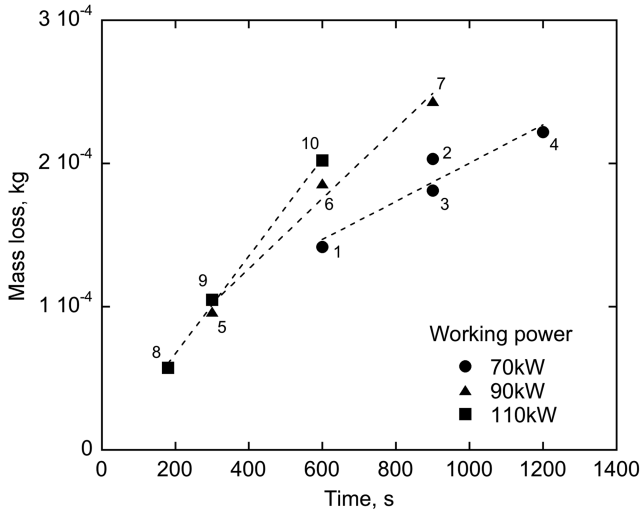

Fig. 6 Comparison of the amount of mass loss of graphite test pieces between different wind-tunnel test conditions.

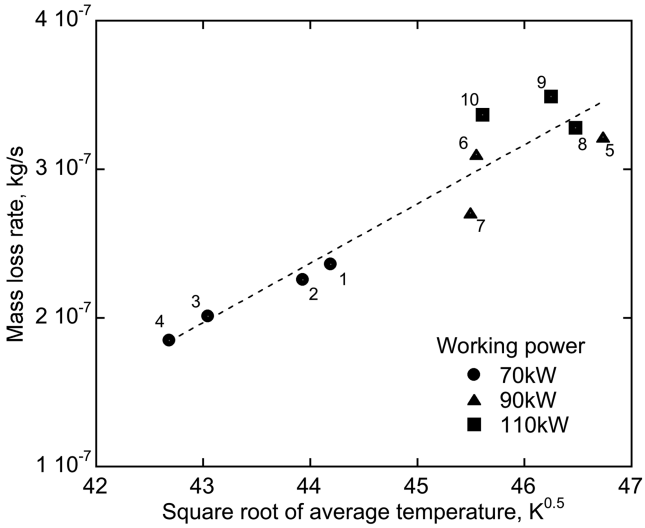

Fig. 7 Mass loss rate of graphite test piece plotted against square root of average surface temperature.

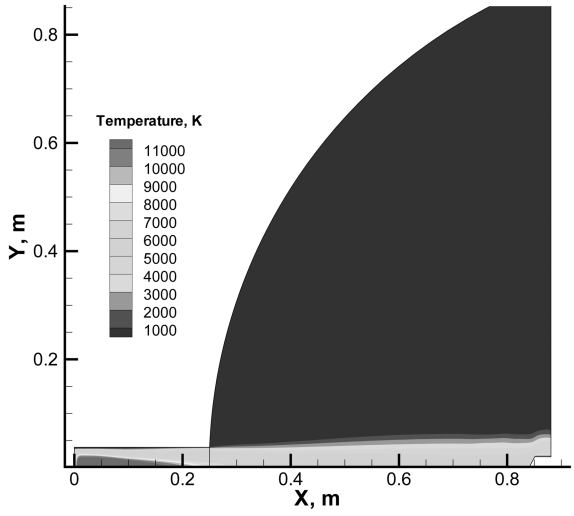

Fig. 8 Typical example of converged solution for the case of 90 kW working power. Temperature contours in zones 1 and 3 are shown.

10,000 K, and then gradually decreases toward the downstream direction.

Calculated temperature, density, and species concentrations along the stagnation stream line in the test chamber are shown in Figs. 9a–9c, respectively. As shown in Fig. 9a, a maximum temperature value of about 7800 K is obtained at the entrance of test chamber, and then gradually decreases toward the test piece. One can also see from Fig. 9a that thermal equilibrium is established in the entire region. Figure 9c represents the mass fraction of atomic and molecular nitrogen. From this figure, one can see that recombination of atomic nitrogen occurs along the stagnation stream line. The mass fraction of atomic nitrogen at the test piece is about 0.21. From Figs. 9b and 9c, atomic nitrogen density at the test piece surface for the present heating condition is estimated to be 1.124×10^{-3} kg/m^3. Similarly, calculated values of atomic nitrogen density for the cases of 70 and 110 kW working power are 8.254×10^{-4} and 1.345×10^{-3} kg/m^3, respectively.

For the purpose of comparison, measured values using an emission spectroscopic method by Fujita et al. [10] are given in the same figures. In the work by Fujita et al., the radiation from the flows in the test section of the ICP heated wind tunnel is observed in the radial direction perpendicular to the freestream direction. The measurements are made at 372 mm from the coil center (at 5 mm from the test piece). By comparing the measured spectrum with that calculated by using the computer code SPRADIAN2, molecular temperature and species concentrations are determined for the nitrogen test flow at the wind-tunnel test condition of 90 kW. As shown in these figures, the agreement between the calculation and the measurement is fairly good.

C. Speed of Nitridation Reaction

The mass loss rate is calculated by using Eq. (2) as a function of the speed of nitridation reaction. In the calculation, the surface area value is set to be its original one (2.43×10^{-4} m^2). The surface temperatures for each of the test pieces are taken from the averaged values obtained in the measurement shown earlier. The atomic nitrogen values are given by the calculated ones. The value for the speed of the nitridation reaction for each of the test pieces can be estimated when the averaged mass loss rate obtained earlier is given in the calculation.

A typical result is presented in Fig. 10 for the case of test piece no. 1. In the figure, the calculated mass loss rate is plotted against the speed of reaction. The values for the surface temperature, the atomic nitrogen density, and the mass loss rate are given in the figure. One can recognize that the intersection of the two lines given in the figure represents the speed of nitridation. From the figure, the speed of reaction is found to be 0.00321. The experimental uncertainty is estimated to be $\pm 3\%$ in the surface temperature and -50% in the surface area. These uncertainties affect the speed of reaction evaluated in the present study by -2% to $+103\%$.

The same procedure is used to obtain the speed of nitridation for other test pieces. The obtained speed of reaction for all test pieces is plotted against reciprocal temperature in Fig. 11. Those values are also found in Table 2. For the purpose of comparison, the reaction probability values obtained by Park and Bogdanoff [8] are given in Fig. 11. The reaction probability for the oxidation reaction, taken from [7], is also shown for reference. From the figure, one can see that the speed of nitridation reaction obtained in this study is smaller than the reaction probability for the oxidation reaction. In addition, the

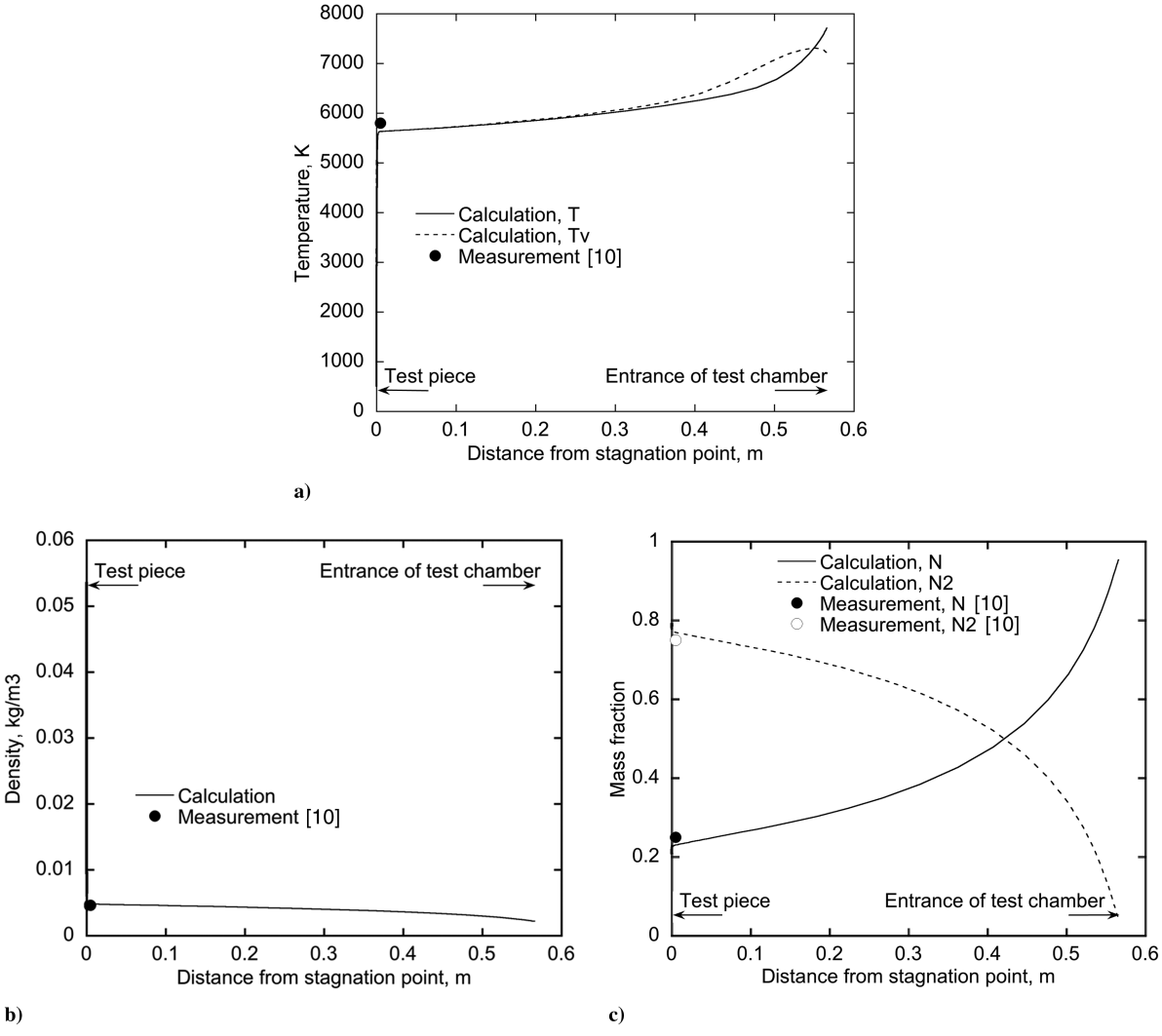

Fig. 9 Flow properties along stagnation stream line for the case of working power of 90 kW: a) temperature, b) density, and c) mass fraction.

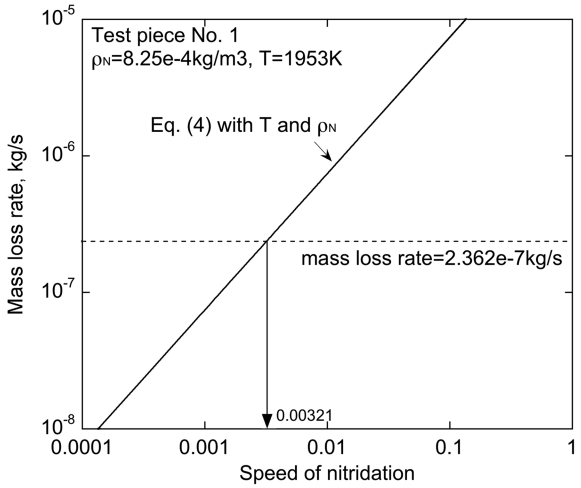

Fig. 10 Mass loss rate of test piece as a function of speed of nitridation for case no. 1.

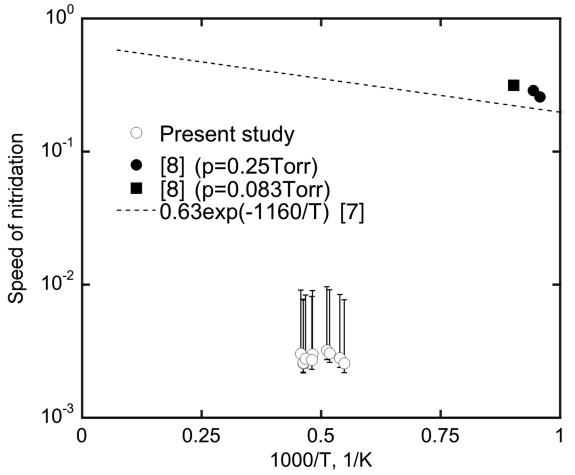

Fig. 11 Speed of nitridation for the present heating environment.

present value is substantially smaller than the probability values obtained by Park and Bogdanoff [8].

V. Discussion

The obtained value for the speed of nitridation in the present study is substantially lower than that obtained by Park and Bogdanoff [8] by a factor of 100. The estimation of the speed of nitridation in the present study is based strongly on the assumption that the surface area and temperature, and the mass density of atomic nitrogen, are constant during the measurement. The present experimental data show that this assumption is likely to be valid, especially for the surface temperature and the area. However, the value of the mass density of the atomic nitrogen onto the graphite surface is unknown in the experiment. Many efforts will be needed to measure the atomic nitrogen value. Therefore, the computed values of the atomic nitrogen are believed to be informative to show what the mass loss data obtained in this study indicate if the accuracy of the calculated flow properties would be acceptable.

There are two major uncertainties in the calculated atomic nitrogen values: the surface temperature and the radial variation of the atomic nitrogen concentration. In the present calculation, the flowfield solution is obtained by assuming a surface temperature of 500 K. The speed of nitridation value is evaluated from the atomic nitrogen value at the stagnation point of the graphite rod by using the flowfield solution. Calculations are made by using a different temperature value of 2000 K, which is the typical temperature value obtained in the present measurements. The result shows that the mass fraction of atomic nitrogen at the stagnation point becomes +5% larger than that obtained by using the surface temperature value of 500 K. On one hand, based on an independent experimental work [11], in which the flows produced by the ICP wind tunnel are characterized using an emission spectroscopic method, it is found that the radial gradient of the flow properties, such as temperature, enthalpy, and the species concentration at the test section, is negligibly small compared to the diameter of the graphite rod. Therefore, the results suggest that the surface temperature and the radial variation of the flow around the rod may have little impact on the evaluated speed of nitridation value.

A further investigation was made very recently, as a sequel to the present study, to examine the effect of the temporal variations of the parameters such as the surface area and temperature, and the mass density of atomic nitrogen [15]. In the work, the thermal response of graphite test pieces under the ICP wind-tunnel condition is calculated in more detail by coupling with the flowfield around the test piece. The result shows the speed of nitridation reaction deduced in this work is not so affected by the temporal variations of those parameters. This result implies that it is unlikely that the uncertainties of the aforementioned parameters are attributed largely to the deduced speed of nitridation.

The reason for the difference between the present study and the one obtained by Park and Bogdanoff [8] remains unknown. Even if the time variation of the nitrogen density is calculated by accounting for a possible physical mechanism, such as the condensation of the atomic carbon produced in the boundary layer on the surface, whether the data obtained by the present method approach the value of the reaction probability given by Park and Bogdanoff is uncertain. Additionally, the present experimental data indicate that if the data given by Park and Bogdanoff would be correct, all of the graphite test pieces considered in the present study would be lost. More experimental data, especially at lower temperatures, will be required to explore a possible cause of the discrepancy between the present and the Park and Bogdanoff values.

VI. Conclusions

Heating tests are conducted in the 110 kW ICP heated wind tunnel in IAT of JAXA. In the tests, graphite test pieces are exposed to nitrogen test flow. Mass loss of the test pieces due to nitridation reaction is successfully measured after the heating tests. A maximum mass loss of about 38% is obtained for the operating conditions of working power of 90 kW. The mass loss data are obtained in a rate-controlled regime. Using the measured mass loss of test pieces and calculated atomic nitrogen density value using a CFD method, the speed of nitridation for the present heating environment is estimated. The calculated value is about 0.003 for a temperature of about 1900 K. It is found that the speed of nitridation obtained in this study is about 1/100 smaller than the reaction probability values obtained by Park and Bogdanoff [8]. More work will be required to find the cause of the difference between the present study and the one given by Park and Bogdanoff.

Acknowledgments

This work was partly supported by the Grant-in-Aid for Young Scientists (B) (No. 18760613) from the Ministry of Education, Culture, Sports, Science, and Technology in Japan. The authors thank Hiroshi Osawa of Tohoku University for valuable discussions, and appreciate various technical suggestions for the experiment given by Takeshi Ito, Keisuke Fujii, Masahito Mizuno, Kiyomichi Ishida, Junsei Nagai, and Masashi Taniguchi of the Wind Tunnel Technology Center of the Japan Aerospace Exploration Agency.

References

[1] Olynick, D., Chen, Y.-K., and Tauber, M. E., "Aerothermodynamics of the Stardust Sample Return Capsule," *Journal of Spacecraft and Rockets*, Vol. 36, No. 3, 1999, pp. 442–462.

[2] Suzuki, T., Furudate, M., and Sawada, K., "Unified Calculation of Hypersonic Flowfield for a Reentry Vehicle," *Journal of Thermophysics and Heat Transfer*, Vol. 16, No. 1, 2002, pp. 94–100.

[3] Suzuki, T., Sakai, T., and Yamada, T., "Calculation of Thermal Response of Ablator Under Arcjet Flow Condition," *Journal of Thermophysics and Heat Transfer*, Vol. 21, No. 2, 2007, pp. 257–266. doi:10.2514/1.25499

[4] Rosner, D. G., and Allendorf, H. D., "Comparative Studies of the Attack of Pyrolytic and Isotropic Graphite by Atomic and Molecular Oxygen at High Temperatures," *AIAA Journal*, Vol. 6, April 1965, pp. 650–654.

[5] Marsh, H., O'Hair, T. E., and Wynnes-Jones, L., "Carbon-Atomic Oxygen Reaction Surface-Oxide Formation on Paracrystalline Carbon and Graphite," *Carbon*, Vol. 7, May 1969, pp. 555–566. doi:10.1016/0008-6223(69)90028-1

[6] Lundell, J. H., and Dickey, R. R., "Ablation of ATJ Graphite at High Temperatures," *AIAA Journal*, Vol. 11, Feb. 1973, pp. 216–222.

[7] Park, C., "Effect of Atomic Oxygen in Graphite Ablation," *AIAA Journal*, Vol. 14, No. 11, 1976, pp. 1640–1642.

[8] Park, C., and Bogdanoff, D. W., "Shock-Tube Measurement of Nitridation Coefficient of Solid Carbon," *Journal of Thermophysics and Heat Transfer*, Vol. 20, No. 3, 2006, pp. 487–492. doi:10.2514/1.15743

[9] Park, C., "Nonequilibrium Air Radiation (NEQAIR) Program: User's Manual," NASA TM-86707, 1985.

[10] Fujita, K., Mizuno, M., Ishida, K., and Ito, T., "Spectroscopic Flow Evaluation in Inductively Coupled Plasma Wind Tunnel," *Journal of Thermophysics and Heat Transfer* (submitted for publication); also *43rd AIAA Aerospace Sciences Meeting and Exhibit*, AIAA Paper 2005-173, Jan. 2005.

[11] Fujita, K., Suzuki, T., Mizuno, M., and Fujii, K., "Comprehensive Characterization of Test Flows in 110-kW Inductively-Coupled-Plasma Heater," *46th AIAA Aerospace Sciences Meeting and Exhibit*, AIAA Paper 2008-1254, Jan. 2008.

[12] Ando, K., Sakai, T., and Yamada, T., "Calculation of Flows in an Inductively Coupled CO_2 Plasma Wind Tunnel," *Symposium on Flight Mechanics and Astrodynamics*, Inst. of Space and Astronautical Sciences, Japan Aerospace Exploration Agency, Kanagawa, Japan, 2006, pp. 17–19 (in Japanese).

[13] Wada, Y., and Liu, M. S., "Flux Splitting Scheme with High Resolution and Robustness for Discontinuities," AIAA Paper 94-0083, Jan. 1994.

[14] Park, C., "Calculation of Stagnation-Point Heating Rates Associated with Stardust Vehicle," *Journal of Spacecraft and Rockets*, Vol. 44, No. 1, 2007, pp. 24–32. doi:10.2514/1.15745

[15] Suzuki, T., Fujita, K., and Sakai, T., "Numerical Study of Graphite Ablation in Nitrogen Flow," *46th AIAA Aerospace Sciences Meeting and Exhibit*, AIAA Paper 2008-1217, Jan. 2008.